Journal of Experimental Botany, Vol. 62, No. 7, pp. 2393–2402, 2011
doi:10.1093/jxb/err034 Advance Access publication 25 March, 2011

Journal of Experimental Botany
www.jxb.oxfordjournals.org

REVIEW PAPER

Electron tomography of plant thylakoid membranes

Bertram Daum and Werner Kühlbrandt*

Max Planck Institute of Biophysics, D-60438 Frankfurt am Main, Germany

* To whom correspondence should be addressed. E-mail: werner.kuehlbrandt@biophys.mpg.de

Received 2 December 2010; Revised 24 January 2011; Accepted 25 January 2011

Abstract

For more than half a century, electron microscopy has been a main tool for investigating the complex ultrastructure and organization of chloroplast thylakoid membranes, but, even today, the three-dimensional relationship between stroma and grana thylakoids, and the arrangement of the membrane protein complexes within them are not fully understood. Electron cryo-tomography (cryo-ET) is a powerful new technique for visualizing cellular structures, especially membranes, in three dimensions. By this technique, large membrane protein complexes, such as the photosystem II supercomplex or the chloroplast ATP synthase, can be visualized directly in the thylakoid membrane at molecular (4–5nm) resolution. This short review compares recent advances by cryo-ET of plant thylakoid membranes with earlier results obtained by conventional electron microscopy.

Key words: cF_1F_o ATP synthase, chloroplast, electron cryotomography, photosystem II, plastoglobules, thylakoid membrane, thylakoid ultrastructure.

Introduction

Chloroplasts are the organelles that carry out photosynthesis in green plants and algae. The conversion of solar energy into chemical energy in the form of ATP and NADPH is accomplished by six major membrane protein complexes: light harvesting complex II and I (LHCII and LHCI), photosystem II and I (PSII and PSI), cytochrome b_6/f (cytb_6/f), and the chloroplast ATP synthase (cF_1F_o-ATP synthase) (Nelson and Ben-Shem, 2004). These complexes are located in the thylakoid membrane (Greek θύλακὸς = sack; Menke, 1962), which is surrounded by the chloroplast stroma and encloses the thylakoid lumen (reviewed by Albertsson, 2001; Staehelin, 2003; Dekker and Boekema, 2005).

Early on, electron microscopy of isolated thylakoids, and of resin-embedded sections of isolated chloroplasts or whole leaves revealed that the thylakoid membrane is a highly folded continuum, differentiated into stacks of appressed, flattened membrane vesicles called thylakoid grana, and non-appressed stroma membranes connecting the grana (Menke, 1960, 1962; Falk and Sitte, 1963; Weier *et al.*, 1963; Wehrmeyer, 1964*a*, *b*).

Electron microscopy of freeze-fracture replicas (Staehelin, 1975; Armond *et al.*, 1977; Machold *et al.*, 1977; Kirchhoff *et al.*, 2007; van Roon *et al.*, 2000), plastic sections (Miller and Staehelin, 1976; Kreuz *et al.*, 1986), and negatively stained samples (Boekema *et al.*, 2000) in conjunction with biochemical studies (Andersson and Anderson, 1980) indicated that the two regions of the thylakoid membrane are not only morphologically, but also functionally distinct. In terms of membrane protein content, the stacked grana thylakoids consist mainly of LHCII and PSII, whereas PSI, LHCI, and the ATP synthase predominantly reside in the unstacked stroma lamellae and grana end membranes. Cytb_6/f was suggested to be present in appressed as well as non-appressed thylakoid regions (reviewed by Albertsson, 2001; Staehelin, 2003; Dekker and Boekema, 2005).

The lateral heterogeneity and functional subcompartmentalization of the thylakoid membrane into stacked grana and non-stacked stroma membranes has been proposed to serve many purposes, including an increase in light-harvesting efficiency (Barber, 1980), to balance the electron flow between PSII and PSI or in preventing spillover of excitation energy from PSII to PSI (Anderson, 1981; Trissl and Wilhelm, 1993), to fine-tune photosynthesis under variable light conditions (Chow *et al.*, 2005), to aid state transitions (Horton and Black, 1980; Chow *et al.*, 1981), or to switch from linear to cyclic electron flow (Chow, 1984).

To understand the interplay between these molecular processes and the morphology of the thylakoid network, it is necessary to know how the photosynthetic complexes are distributed in their native membrane environment. The development of electron cryo-tomography gives new insights into the three-dimensional (3D) organization of large protein complexes *in situ* and is therefore an ideal tool to provide a deeper understanding of thylakoid organization.

Electron cryotomography

Electron tomography (ET) makes it possible to image biological specimens in three dimensions in the electron microscope on the nanometre scale (for recent reviews, see Bárcena and Koster, 2009; Pierson *et al.*, 2009; Ben-Harush *et al.*, 2010; Tocheva *et al.*, 2010). 3D information is collected by recording series of tilted projections in increments of 1–5° in a range of ±70°. In the computer, the images of each tilt series are projected back into a 3D volume (Baumeister *et al.*, 1999). For conventional ET, samples are embedded in plastic and sectioned by ultramicrotomy. Although this yields high-contrast images of gross cellular features including membranes, molecular detail is lost. To obtain tomograms of 4–5nm resolution (Leis *et al.*, 2009), the sample has to be vitrified (Dubochet *et al.*, 1988) and examined by electron cryo-tomography (cryo-ET). Samples for cryo-ET are prepared by spreading solutions of protein complexes, viruses, suspensions of small bacteria, or even thin eukaryotic cells on an electron microscopy (EM) grid coated with a holey carbon film. A thin film of suspension forms in the holes, and is rapidly frozen in liquid ethane. Larger samples, such as cells or tissues, are frozen under high pressure and then sectioned by cryo-ultramicrotomy (Al-Amoudi *et al.*, 2004; Norlen *et al.*, 2009). This is also necessary for whole chloroplasts, which are too large for cryo-ET of organelle suspensions. As vitreous sections are susceptible to mechanical damage, melting, and contamination, cryo-ET of such sections is a demanding technique that is not practised in many laboratories. Studying a large number of samples under many different conditions by this approach would be difficult. As an alternative, whole chloroplasts can be spread on the EM grid and then vitrified by plunging into liquid ethane. When the grid is blotted to create a thin layer of suspension for freezing, most of the chloroplasts rupture due to surface tension. This method maintains the thylakoid network as well as the lateral heterogeneity between stroma and grana thylakoids (Daum *et al.*, 2010), and is therefore suitable for studying the arrangement of membrane proteins within them.

Three-dimensional organization of the thylakoid membrane

The first models of the 3D organization of the thylakoid membrane were proposed in the early 1960s (Menke, 1960; Heslop Harrison, 1963; Weier *et al.*, 1963; Wehrmeyer, 1964*a*, *b*). Since then, several different 3D models of grana and stroma thylakoids have been proposed (reviewed by Mustárdy and Garab, 2003; Nevo *et al.*, 2009). Evidence accumulated that thylakoids comprise a fretwork of stroma lamellae, which wind around the grana stacks as a right-handed helix, connecting individual grana disks by narrow membrane protrusions (Fig. 1A). This model was derived by combining images of resin-embedded sections with top views of isolated thylakoid networks (Wehrmeyer, 1964*a*, *b*). It received support by EM of serial plastic sections (Paolillo, 1970; Brangeon and Mustárdy, 1979), scanning electron microscopy (Mustárdy and Janossy, 1979), freeze fracture EM (Staehelin, 1986), and ET on plastic sections of isolated thylakoids (Mustárdy *et al.*, 2008). While this model has been widely accepted, it has also been criticized for not allowing the extensive reorganization of thylakoid

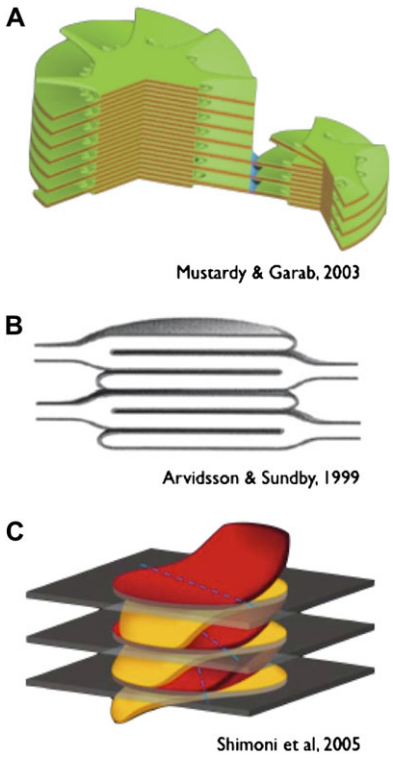

Fig. 1. Models of thylakoid organization. (A) The helix model (Mustárdy and Garab, 2003, with permission) postulates a fretwork of stroma lamellae, which wind around the grana stacks as a right-handed helix, connecting to individual grana disks by narrow membrane protrusions. (B) The simpler model of Arvidsson and Sundby [1999 (with the permission of CSIRO Publishing;http://www.publish.csiro.au/nid/102/paper/PP99072.htm)] suggests that a grana stack consists of repetitive units, each containing three grana disks formed by symmetrical invaginations of a thylakoid pair. (C) In the model of Shimoni *et al.* [2005 (Copyright American Society of Plant Biologists), with permission] the grana disks are paired units emerging from bifurcations of stroma thylakoids. A pair of disks is formed by a bifurcation of a lamellar stroma thylakoid in the cylinder of stacked grana membranes. In each pair, the upper disk bends upwards to fuse with next pair in the stack, and the lower disk bends down on the opposite side to fuse with the disk below.

membranes that is known to happen under changing light conditions (Arvidsson and Sundby, 1999). Instead, a less complex alternative model based on EM of plastic-embedded sections was proposed (Fig. 1B) (Arvidsson and Sundby, 1999). In this simpler model, a granum is composed of piles of repetitive units, each containing three grana discs, which are formed by symmetrical invaginations of a thylakoid pair.

Another model of thylakoid organization in chloroplasts was based on electron tomography of thin plastic sections of freeze-substituted material (Shimoni *et al.*, 2005). In this model, the grana disks were presented as paired units formed by bifurcation of stroma thylakoids. A pair of disks is formed by a bifurcation of a lamellar stroma thylakoid in the cylinder of stacked grana membranes. In each pair, the upper disk bends upwards to fuse with the next pair in the stack, and the lower disk bends down on the opposite side to fuse with the disk below (Shimoni *et al.*, 2005) (Fig. 1C). This model contradicted the established helix model (Paolillo, 1970) and has been much debated in the recent literature (Brumfeld *et al.*, 2008; Mustárdy *et al.*, 2008).

The first cryo-ET study of vitreous chloroplast sections (Daum *et al.*, 2010) presented a segmented volume of the grana–stroma interface of five grana lamellae (Fig. 5B). In vitrified sections, which represent the native, undisturbed state of the thylakoid membrane, grana are seen as stacks of straight, exactly parallel membranes. The 3D surface representation in the study by Daum *et al.* (2010) shows that each grana disk consists of a pair of planar membranes, in contrast to the model by Shimoni *et al.* (2005), where grana disks bend up or down to merge with the next membrane in the stack. The 3D volume of vitrified sections did not show any bending of grana thylakoids or internal connections between successive grana disks, as reported by Shimoni *et al.* (2005). Instead, pairs of grana disks merge with stroma lamellae at the grana margins by staggered membrane protrusions, rather than by a simple bifurcation. The plane of the stroma membranes is tilted relative to the plane of grana by ~10–15°, so that the stroma lamellae ascend around the grana stack in a right-handed fashion, connecting consecutive grana disks by fret-like membrane protrusions. These observations are entirely consistent with the helix model (Paolillo, 1970; Mustárdy *et al.*, 2008).

In their supplementary movie, Daum et al. (2010) also presented a cryo-tomogram of a whole chloroplast ruptured on the EM grid shortly before it was frozen in liquid ethane. The tomographic volume contained an entire thylakoid network, consisting of cylindrical grana stacks interconnected by unstacked stroma thylakoids, suggesting that the chloroplast ultrastructure had been largely preserved. The segmented and surface-rendered tomographic volume, containing two grana stacks which merge at their margins with several unstacked stroma thylakoids, is shown in Fig. 2. The grana stacks have the expected cylindrical shape, measuring ~500nm in diameter and 130–160nm in height. Due to the missing wedge effect (Frank, 2006), membranes parallel to

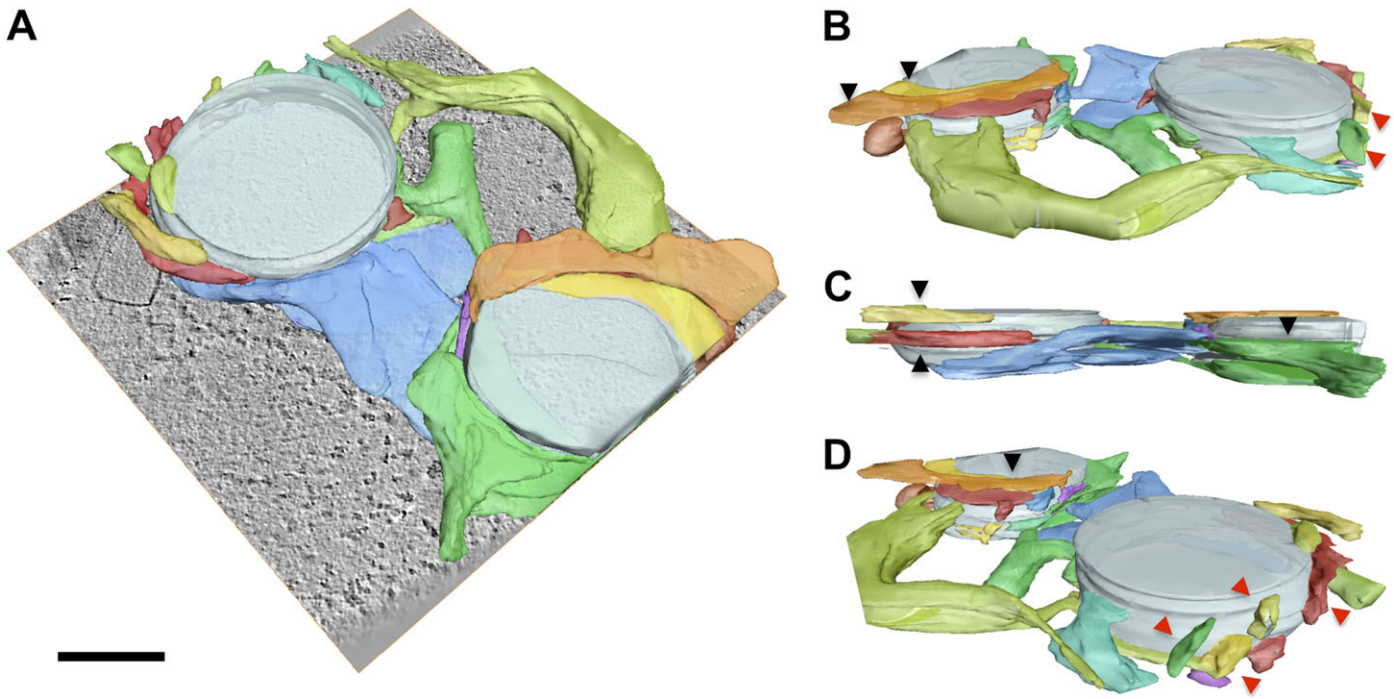

Fig. 2. Tomographic surface representation of the thylakoid network within a ruptured chloroplast. (A) Segmented cryo-ET of a freshly ruptured, rapidly frozen chloroplast showing two grana stacks (translucent grey) interconnected by a network of stroma thylakoids (multiple colours). The grana stacks are drawn as solid cylindrical bodies, since individual membranes within a stack are not clearly resolved, due to the missing wedge effect (see text). Scale bar: 200nm. (B–D) The same segmented volume seen from three different angles. Stroma thylakoids merging with one grana disk in one plane are indicated by black arrowheads; those that connect to several disks in a grana stack are indicated by red arrowheads.

the EM grid plane were not well resolved. Nevertheless, the number of grana thylakoids within each stack was determined by the repeating layers of PSII dimers, which were clearly visible. In this way, it was possible to discriminate six or eight successive membrane layers in two of the grana stacks, corresponding to three or four grana disks, respectively.

Most stroma thylakoids extended out of the tomographic volume and could therefore not be traced from one granum to the next. However, several stroma membranes connected the two grana stacks to one another. All connecting stroma thylakoids branched to fuse with at least two different disks in the neighbouring grana stack. At the interface between grana and stroma thylakoids, two different types of connections were observed: some stroma thylakoids merged with only one grana disk in the plane of the membrane pair, wrapping partly around the margin of the grana stack (Fig. 2B–D). Other stroma lamellae fused with several grana disks within one stack, including an angle between <10° and 50° with the disks (Fig. 2B, D). Although the slope of the connecting stroma membranes varied over a wider range than previously observed, it was always right handed, ascending counter-clockwise (from left to right) around the circumference of the grana stack.

There was no evidence in the tomographic volume of the two grana stacks and connecting stroma membranes that the thylakoid network was in any way disrupted. The segmented volume thus showed that the previous models in Fig. 1A–C are idealized interpretations of reality. In particular, the grana–stroma assembly was much less regular than suggested by most models. Apart from that, these tomographic data support certain aspects of the helix model (Mustárdy and Garab, 2003) in that the stroma thylakoids run at an angle relative to the grana disks and follow the periphery of a grana stack in a right-handed helix. It is found, however, that only some, but not all of the stroma thylakoids follow this rule and connect to more than one disk in a stack, while others fuse with only one grana disk in one plane.

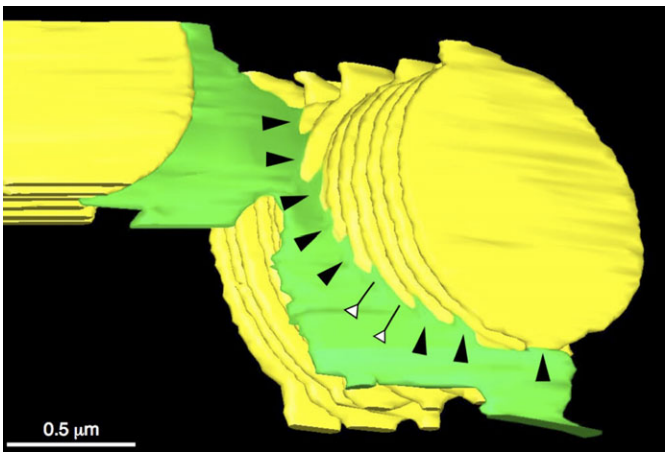

Fig. 3. Tomographic surface representation of grana and stroma thylakoids from freeze-substituted chloroplast sections. Two grana thylakoid stacks (yellow) are interconnected by a stroma thylakoid (green). The stroma thylakoid winds around the grana stack (on the right) in a right-handed helical fashion connecting nine consecutive grana disks with each other by fret-like membrane protrusions [Austin and Staehelin, 2011 (Copyright American Society of Plant Biologists) with permission].

Very recently, ET and serial sections of freeze-substituted chloroplasts revealed the organization of thylakoid networks around grana stacks *in situ* (Fig. 3) (Austin and Staehelin, 2011). The findings of these authors also support the helical model (Paolillo, 1970; Mustárdy *et al.*, 2008). by showing that stroma thylakoids indeed wind around grana thylakoids as a right-handed helix, including an angle of 20–25° with the grana membranes, and connecting to successive grana pairs by staggered, fret-like protrusions. Similar to our findings (Fig. 2), Austin and Staehelin (2011) showed that the architecture of the thylakoid network is more variable than presented in the model by Mustárdy *et al.* (2008). Whereas some stroma thylakoids merge with successive grana disks in short, ~35nm wide, slit-like junctions, other junctions are up to 400nm wide, so that one stroma thylakoid forms a planar sheet with only one grana disk. As in tomograms of vitrified sections (Daum *et al.*, 2010), the grana disks in a stack are completely flat, with no sign of out-of-plane bending, or fusion with appressed grana disks (Fig. 1D).

Taken together, the tomographic data presented by Daum *et al.* (2010), Austin and Staehelin (2011), and here show that the helix model of thylakoid membrane architecture in chloroplasts is correct. Other models do not describe this architecture correctly and can now be safely discarded.

Plastoglobules

Plastoglobules are small (~45–60nm), lipid-filled vesicles in chloroplasts thought to be surrounded by a single membrane leaflet (Austin *et al.*, 2006). Plastoglobules contain plastid-specific lipids such as monogalactosyl diacylglycerol, digalactosyl diacylgycerol, triacylglycerols, free fatty acids, tocopherols, plastoquinone, and menaquinones (Lichtenthaler, 1968; Steinmüller and Tevini, 1985; Tevini and Steinmüller, 1985; Ghosh *et al.*, 1994; Kaup *et al.*, 2002). They also contain a number of proteins in their boundary single-leaflet membrane, including proteins of the PAP/fibrillin family, which appear to be plastoglobule specific (Deruere *et al.*, 1994; PozuetaRomero *et al.*, 1997; Kessler *et al.*, 1999). Plastoglobules are involved in plastid lipid biosynthesis (Vidi *et al.*, 2006; Ytterberg *et al.*, 2006), and are particularly abundant during chloroplast greening (Lichtenthaler and Tevini, 1970; Tevini *et al.*, 1977) or leaf senescence (Tevini and Steinmüller, 1985).

In 2006, Austin and co-workers published a study on the association of plastoglobules with thylakoid membranes in plastic sections of freeze-substituted chloroplasts (Fig. 4). The authors showed that the plastoglobules occur as single entities or in small groups. In young chloroplasts, most plastoglobules were single, but they were more abundant and interconnected into groups during senescence. The plastoglobules are physically attached to the thylakoid membrane and

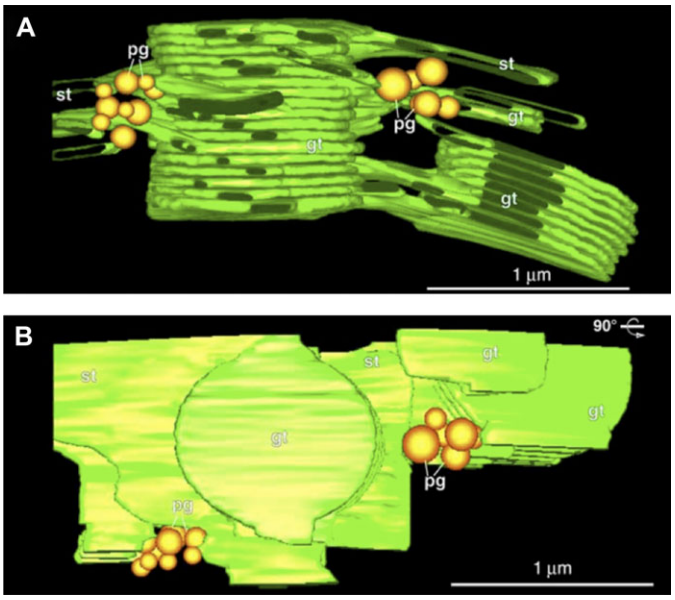

Fig. 4. Grana and stroma thylakoids and plastoglobules. Surface representation of grana (gt) and stroma thylakoids (st) with plastoglobules (pg) seen edge-on (A), or from the top (B) in a tomogram of a thin section through a high-pressure frozen, plastic-embedded chloroplast [from Austin *et al.*, 2006 (Copyright American Society of Plant Biologists) with permission]. Thylakoid membranes are green. Plastoglobules (yellow spheres) are attached to highly curved regions of unstacked stroma thylakoids.

do not float freely in the stroma, as had been suggested (Hansmann and Sitte, 1982). Thylakoid attachment is consistent with reports that plastoglobules are part of the thylakoid network (Yao *et al.*, 1991*a*, *b*; Ghosh *et al.*, 1994) rather than the chloroplast inner envelope, as had been proposed earlier (Kessler *et al.*, 1999). Tomographic data (Austin *et al.*, 2006) also support the notion that plastoglobules are blisters of the outer thylakoid membrane leaflet. The observation that they were associated with highly curved regions of the thylakoid membrane suggested that membrane curvature may be important for their formation.

By immunugold labelling of high-pressure frozen and freeze-substituted chloroplasts, Austin *et al.* (2006) were able to localize plastoglobin PGL-35 and tocopherol cyclases VTE 1 in plastoglobules of *Arabidospis thaliana*. The labelling experiments thus confirmed that these proteins are plastoglobule specific and do not occur elsewhere in the chloroplast. Moreover, these experiments suggested that VTE1 and PGL35 both sit in the half-membrane that surrounds the plastoglubules and extend into the plastoglobule interior.

Thylakoid membranes *in situ* at molecular resolution

Lateral heterogeneity

Cryo-ET of frozen-hydrated chloroplast sections (Daum *et al.*, 2010) (Fig. 5A) and of isolated thylakoid membranes (Daum *et al.*, 2010; Dudkina *et al.*, 2010*a*; Kouril *et al.*, 2011) (Fig. 5C–F) provide clear support for the long-established theory of lateral heterogeneity between stacked and unstacked thylakoids (reviewed by Dekker and Boekema, 2005). Tomograms of vitreous sections showed PSII densities protruding into the lumen of stacked grana thylakoids, whereas these densities were not visible in unstacked stroma thylakoids (Daum *et al.*, 2010) (Fig. 5A). Grana stacks isolated by mild detergent treatment (Daum *et al.*, 2010; Dudkina *et al.*, 2010*a*; Kouril *et al.*, 2011) and stacks in whole chloroplasts ruptured on the EM grid (Daum *et al.*, 2010) (Fig. 5C–F) indicated the same distribution of PSII dimers (Fig. 5F) and ATP synthases (Fig. 5C, E). The unstacked thylakoid regions are studded with unidentified protein complexes, which most probably include PSI and/or cyt b_6f (Fig. 5D).

Chloroplast ATP synthases

The same tomographic volumes (Daum *et al.*, 2010) also confirmed that the chloroplast ATP synthase is confined to grana end membranes and stroma thylakoids, but absent from appressed grana membranes (Fig. 5A, C, E), as already suggested by Miller and Staehelin (1976). The chloroplast ATP synthase is almost entirely monomeric and confined to minimally curved membranes. In contrast to Wollenberger *et al.* (1994) or the model proposed by Albertsson and co-workers (2001), no ATP synthases are visible in the highly curved grana margins.

The random distribution of the monomeric chloroplast ATP synthase is in marked contrast to the long rows of ATP synthase dimers, which are a characteristic feature of mitochondrial cristae (Allen *et al.*, 1989; Strauss *et al.*, 2008; Dudkina *et al.*, 2010*b*). The dimer rows are confined to highly curved cristae regions (Strauss *et al.*, 2008). Moreover, there is evidence that the mitochondrial ATP synthase shapes the cristae. Single-particle EM of isolated dimers from *Polytomella* (Dudkina *et al.*, 2005) and yeast (Couoh-Cardel *et al.*, 2010) revealed particles with a characteristic angular shape, in which the F_o parts are closer together than the F_1 parts. When the dimer-specific ATP synthase subunits *e* and *g* are deleted in yeast, the cristae adopt an abnormal, onion-like structure with low membrane curvature (Paumard *et al.*, 2002).

The obvious difference in ATP synthase organization in both organelles suggests that ATP synthase dimer rows are an evolutionary advantage for mitochondria but not for chloroplasts. It has been suggested that this relates to the different pH conditions across the inner mitochondrial membrane or the thylakoid membrane of mitochondria or chloroplasts, respectively (Strauss *et al.*, 2008; Daum *et al.*, 2010). The lack of angular ATP synthase dimers at the highly curved grana margins in chloroplasts also indicates that chloroplasts and mitochondria have developed different mechanisms to maintain the organization of their energy-converting membrane systems.

Photosystem II

Apart from the ATP synthase, the 3D arrangement of PSII in grana stacks was examined in cryo-tomograms (Daum

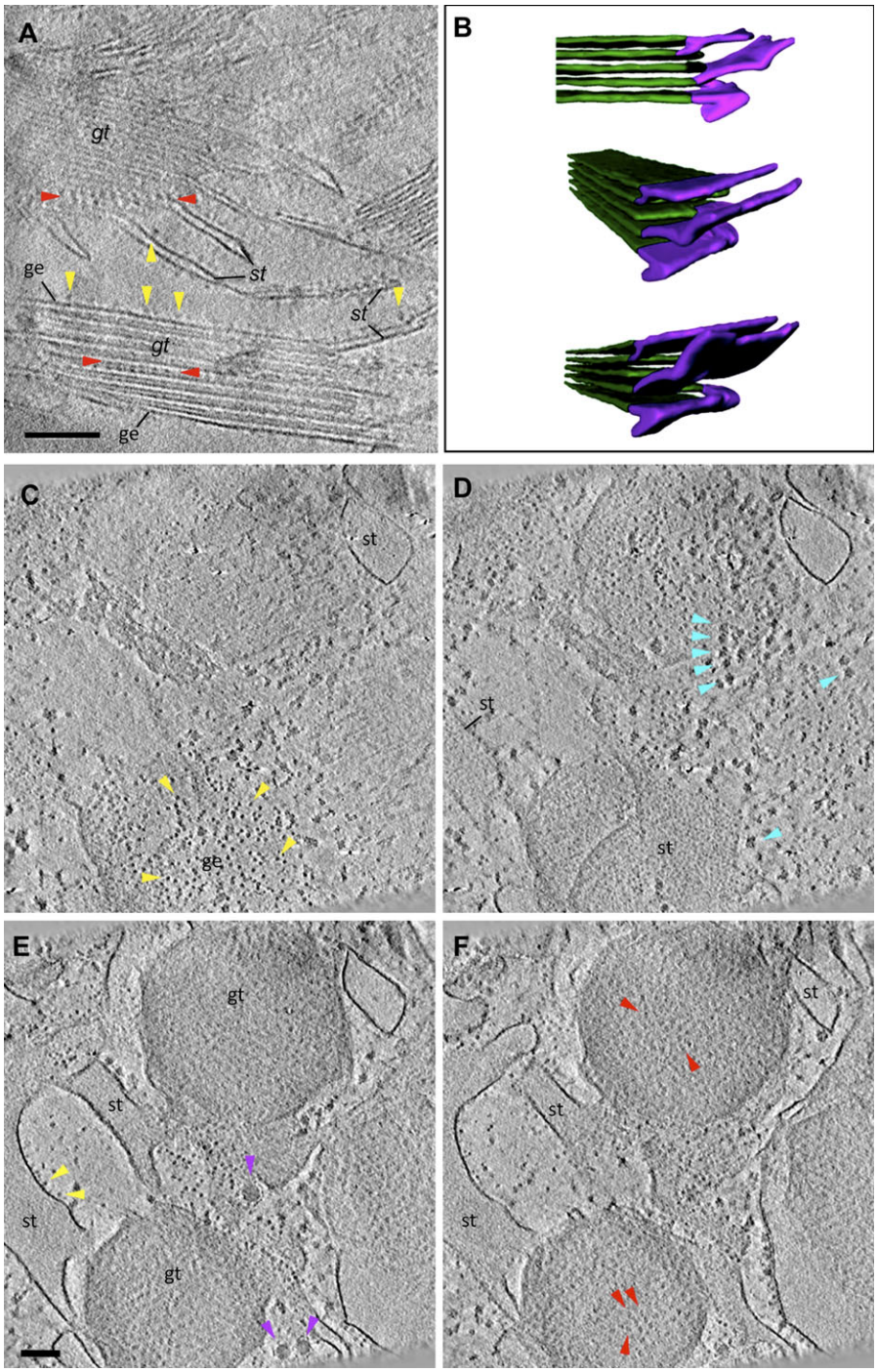

Fig. 5. Cryo-ET of a thylakoid network. (A) Slice through a tomographic volume of a vitreous section of an isolated spinach chloroplast. Parallel straight membranes of stacked grana thylakoids (gt) and unstacked stroma thylakoid membranes (st) are clearly distinguished. ATP synthases (yellow arrowheads) protrude from the flat regions of grana end membranes (ge) and unstacked stromal thylakoids into the stroma. Regular arrays of PSII supercomplexes are visible in some grana membranes (red arrowheads). (B) Tomographic surface representation of the grana–stroma interface in the vitreous chloroplast section shown in A. For simplicity each thylakoid is depicted as a solid slab. The grana discs (green) merge with stroma lamellae (purple) at the grana margins by staggered membrane protrusions, rather than by simple bifurcation. The staggered connections are consistent with the helix model of thylakoid membrane organization (Mustárdy and Garab, 2003) shown in Fig. 1A. (C–F) A sequence of slices through the tomogram of a freshly ruptured chloroplast shown in Fig. 2, parallel to the EM grid plane. Two roughly circular grana thylakoid stacks (gt) with numerous PSII dimers (red arrowheads in F) in a stack of eight (top) or six (below) successive membrane layers are interconnected by several stroma thylakoids (st). Stroma thylakoids (st) and grana end membranes (ge) are studded with cF_1F_o ATP synthase molecules (yellow arrowheads). (D) The tomographic section cuts through the membranes of several stroma thylakoids (st), either in cross-section (left) or tangentially (below). The membranes are speckled with unidentified membrane protein complexes, most probably including PSI and cyt b_6/f. Other regions of the tomogram show

large, dense particles of the shape and size of chloroplast ribosomes (blue arrowheads). Spherical uniform densities are assigned to plastoglobules (purple arrowheads). Redrawn with permission from the supplementary movie in Daum *et al.* (2010) (Copyright American Society of Plant Biologists). Scale bars: 100nm

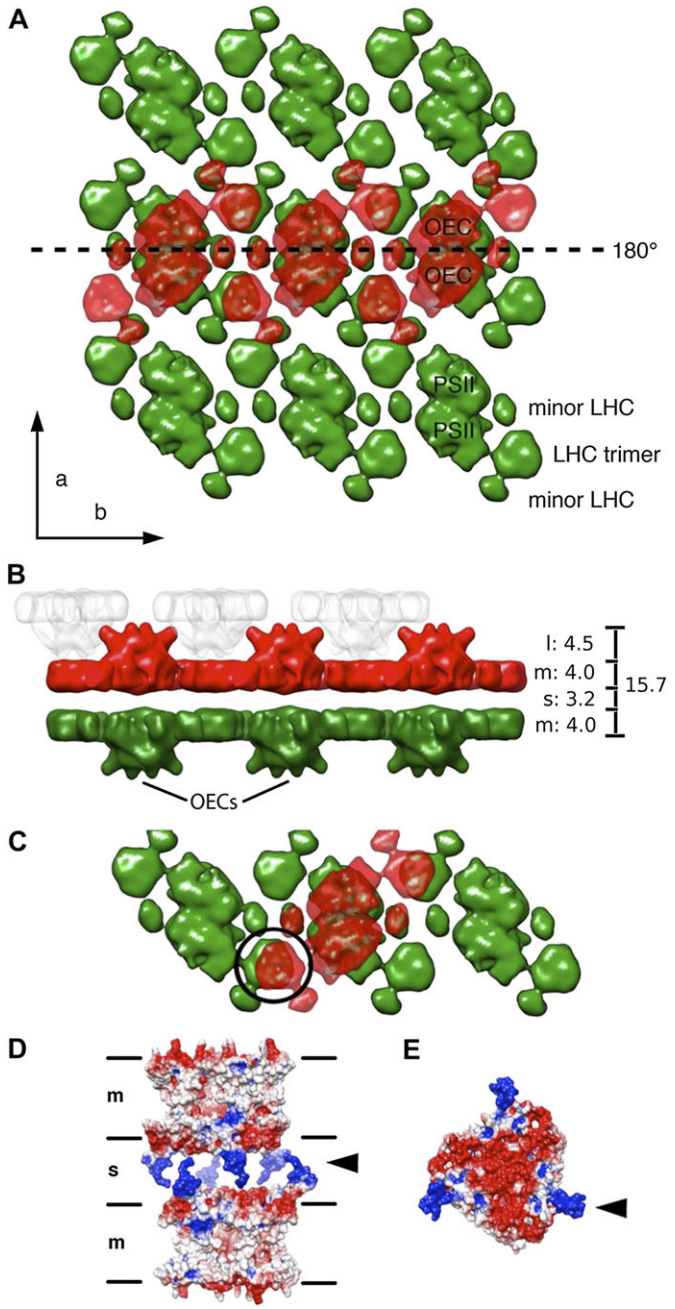

Fig. 6. Interaction of PSII–LHCII supercomplexes in crystalline arrays indicates an electrostatic mechanism of granal stacking. (A) 3D map of the PSII–LHCII supercomplex (Nield and Barber, 2006) at 3nm resolution fitted to PSII lattices in two successive appressed grana membranes. The two lattices are in close contact through their flat stromal surfaces. The lower (green) and upper lattice (red) are related by an in-plane 2-fold axis (dashed line). Oxygen-evolving complexes (OECs) project into the lumenal space, so that the PSII dimers, LHCII trimers, and minor LHCs each interact with another complex of the same kind in the opposite membrane. Black arrows indicate the crystal axes *a* and *b* of the 2D array. (B) Side view of A. The bar on the right indicates the distances (in nm) within the stack. L, lumenal gap; m, membranes; s, stromal gap. OECs of the PSII complexes in one grana disk (red and grey) interdigitate. (C) Detailed view showing how a single supercomplex (red) connects to three others (green) in the opposite membrane. (D) Electrostatic surfaces calculated from the X-ray structure (Standfuss *et al.*, 2005) of LHCII trimers at pH 8.0 in the arrangement in the interacting PSII arrays (black circle in C). The modelled, positively charged N-termini (blue) of one trimer interact with the negatively charged stromal surface (red) of the opposite trimer. Membranes (m) and stromal gap (s) are indicated. (E) Charge distribution on the stromal surface of one LHCII trimer. Black arrowheads in D and E indicate the positively charged N termini [from Daum *et al.*, 2010 (Copyright American Society of Plant Biologists) with permission].

et al., 2010; Dudkina *et al.*, 2010*a*; Kouril *et al.*, 2011). PSII particles were mostly dimers, densely packed in stacked grana membranes. The dense packing typical for the stacked grana regions was not observed in unstacked stroma lamellae. These observations confirmed the widely accepted lateral heterogeneity of membrane protein complexes in the thylakoid membrane (Fig. 5).

Subtomogram averaging of PSII particles within detergent-treated grana membranes resolved the membrane-extrinsic oxygen-evolving complexes (OECs) at ~40Å resolution (Kouril *et al.*, 2011). Due to lack of contrast in the membrane, the intrinsic domains of PSII or LHCII, which are associated with PSII in a PSII–LHCII supercomplex (Nield and Barber, 2006; Caffarri *et al.*, 2009), were not resolved. However, these averages revealed additional lumenal densities on top of the positions expected to be occupied by the LHCII trimers within the PSII–LHCII supercomplex (Kouril *et al.*, 2011). The authors suggested that these additional densities might comprise the violaxanthin de-epoxidase (VDE), an enzyme involved in non-photochemical quenching (Kouril *et al.*, 2011). Further investigations are needed to support this suggestion.

PSII crystals

Crystalline arrays of PSII in grana thylakoids have been described occasionally. Until recently, these arrays were thought to be confined to particular plant mutants, growth conditions, or induced by incubation of isolated thylakoids with particular ionic conditions (reviewed by Dekker and Boekema, 2005). The tomographic volumes of Daum *et al.* (2010) indicate that the PSII arrays occur under normal growth conditions in wild-type market spinach, both in whole, cryo-sectioned chloroplasts and in isolated thylakoid stacks. The crystalline arrays consisted of two layers of PSII in two adjacent thylakoid vesicles, which were in close contact with each other across the stromal gap. By

fitting a molecular model of the PSII–LHCII supercomplex (Nield and Barber, 2006) to the averaged tomographic volume, a model showing the arrangement of supercomplexes in the crystalline lattice was obtained (Fig. 6; Daum *et al.*, 2010). In this model, contacts between PSII–LHCII supercomplexes in both membranes were mediated by the stromal contacts between LHCs and the PSII reaction centre dimers of adjacent membranes. In this arrangement, the LHCII trimers, as well as the minor LHCs within one supercomplex sit on top of the LHCII trimers in the opposite membrane, such that each supercomplex in one membrane spans three rows of supercomplexes in the other. The stromal gap accommodates the N-terminal peptides of LHCII, which are positively charged. In the arrangement entailed by the crystalline membrane model, the N-terminal peptides of two adjacent LHCII trimers happen to interdigitatate and interact with negatively charged surfaces of the opposite LHCII trimer, consistent with the strong electrostatic interactions between appressed grana thylakoids (Barber, 1982). It is likely that LHCII trimers also mediate similar electrostatic interactions between PSII supercomplexes in normal, non-crystalline grana thylakoids, highlighting the fundamental role of LHCII interactions in grana stacks.

Future prospects

EM is currently the only technique able to visualize the macromolecular organization of chloroplasts and their membrane systems in three dimensions. Novel super-resolution light microscopy techniques such as SIM, STED, STORM, or PALM are not likely to achieve the required resolution in the near future (Schermelleh *et al.*, 2010). Although chloroplasts and isolated thylakoid membranes have been studied by EM for more than half a century, the comparatively recent technique of cryo-ET has revealed some surprising new features. Still, some unanswered questions remain, mostly related to the changes in membrane organization and composition in different functional states. Cryo-ET is the ideal technique for studying the variation in macromolecular organization of the thylakoid membrane in response to different environmental or physiological conditions. In principle, this can be done by high-pressure freezing of chloroplast suspensions or even whole leaves, followed by freeze substitution, or even with serial cryo-sections of vitrified samples. A simpler alternative would be to vitrify whole chloroplasts ruptured on the EM grid immediately before they are shock-frozen in liquid ethane, as in the study by Daum *et al.* (2010). This method largely preserves both the lateral heterogeneity of the membranes, and their organization into stacked and unstacked thylakoids. This comparatively straightforward method would allow 'high-throughput' tomographic data collection of chloroplast membranes in different functional states.

References

Al-Amoudi A, Chang JJ, Leforestier A, McDowall A, Salamin LM, Norlen LPO, Richter K, Blanc NS, Studer D, Dubochet J. 2004. Cryo-electron microscopy of vitreous sections. *EMBO Journal* **23,** 3583–3588.

Albertsson PA. 2001. A quantitative model of the domain structure of the photosynthetic membrane. *Trends in Plant Science* **6,** 349–354.

Allen RD, Schroeder CC, Fok AK. 1989. An investigation of mitochondrial inner membranes by rapid-freeze deep-etch techniques. *Journal of Cell Biology* **108,** 2233–2240.

Anderson JM. 1981. Consequences of spatial separation of photosystem-1 and photosystem-2 in thylakoid membranes of higher-plant chloroplasts. *FEBS Letters* **124,** 1–10.

Andersson B, Anderson JM. 1980. Lateral heterogeneity in the distribution of chlorophyll–protein complexes of the thylakoid membranes of spinach-chloroplasts. *Biochimica et Biophysica Acta* **593,** 427–440.

Armond PA, Staehelin LA, Arntzen CJ. 1977. Spatial relationship of photosystem-I, photosystem-II, and light-harvesting complex in chloroplast membranes. *Journal of Cell Biology* **73,** 400–418.

Arvidsson PO, Sundby C. 1999. A model for the topology of the chloroplast thylakoid membrane. *Australian Journal of Plant Physiology* **26,** 687–694.

Austin JR, Frost E, Vidi PA, Kessler F, Staehelin LA. 2006. Plastoglobules are lipoprotein subcompartments of the chloroplast that are permanently coupled to thylakoid membranes and contain biosynthetic enzymes. *The Plant Cell* **18,** 1693–1703.

Austin JR, Staehelin LA. 2011. Three-dimensional architecture of grana and stroma thylakoids of higher plants as determined by electron tomography. *Plant Physiology* (in press).

Barber J. 1980. An explanation for the relationship between salt-induced thylakoid stacking and the chlorophyll fluorescence changes associated with changes in spillover of energy from photosystem-II to photosystem-I. *FEBS Letters* **118,** 1–10.

Barber J. 1982. Influence of surface-charges on thylakoid structure and function. *Annual Review of Plant Physiology and Plant Molecular Biology* **33,** 261–295.

Bárcena M, Koster A. 2009. Electron tomography in life science. *Seminars in Cell and Developmental Biology* **20,** 920–930.

Baumeister W, Grimm R, Walz J. 1999. Electron tomography of molecules and cells. *Trends in Cell Biology* **9,** 81–85.

Ben-Harush K, Maimon T, Patla I, Villa E, Medalia O. 2010. Visualizing cellular processes at the molecular level by cryo-electron tomography. *Journal of Cell Science* **123,** 7–12.

Boekema EJ, van Breemen JFL, van Roon H, Dekker JP. 2000. Arrangement of photosystem II supercomplexes in crystalline macrodomains within the thylakoid membrane of green plant chloroplasts. *Journal of Molecular Biology* **301,** 1123–1133.

Brangeon J, Mustárdy L. 1979. The ontogenetic assembly of intra-chloroplastic lamellae viewed in 3-dimension. *Biologie Cellulaire* **36,** 71–80.

Brumfeld V, Charuvi D, Nevo R, Chuartzman S, Tsabari O, Ohad I, Shimoni E, Reich Z. 2008. A note on three-dimensional models of higher-plant thylakoid networks. *The Plant Cell* **20,** 2546–2549.

Caffarri S, Kouril R, Kereiche S, Boekema EJ, Croce R. 2009. Functional architecture of higher plant photosystem II supercomplexes. *The EMBO Journal* **28,** 3052–3063.

Chow WS. 1984. The extent to which the spatial separation between photosystems-I and photosystems-II associated with granal formation limits noncyclic electron flow in isolated lettuce chloroplasts. *Archives of Biochemistry and Biophysics* **232,** 162–171.

Chow WS, Kim EH, Horton P, Anderson JM. 2005. Granal stacking of thylakoid membranes in higher plant chloroplasts: the physicochemical forces at work and the functional consequences that ensue. *Photochemical and Photobiological Sciences* **4,** 1081–1090.

Chow WS, Telfer A, Chapman DJ, Barber J. 1981. State 1–State 2 transition in leaves and its association with ATP-induced chlorophyll fluorescence quenching. *Biochimica et Biophysica Acta* **638,** 60–68.

Couoh-Cardel SJ, Uribe-Carvajal S, Wilkens S, Garcia-Trejo JJ. 2010. Structure of dimeric F1F0-ATP synthase. *Journal of Biological Chemistry* **285,** 36447–36455.

Daum B, Nicastro D, Austin JR, McIntosh JR, Kühlbrandt W. 2010. Arrangement of photosystem II and ATP synthase in chloroplast membranes of spinach and pea. *The Plant Cell* **22,** 1299–1312.

Dekker JP, Boekema EJ. 2005. Supramolecular organization of thylakoid membrane proteins in green plants. *Biochimica et Biophysica Acta* **1706,** 12–39.

Deruere J, Romer S, Dharlingue A, Backhaus RA, Kuntz M, Camara B. 1994. Fibril assembly and carotenoid overaccumulation in chromoplasts—a model for supramolecular lipoprotein structures. *The Plant Cell* **6,** 119–133.

Dubochet J, Adrian M, Chang JJ, Homo JC, Lepault J, Mcdowall AW, Schultz P. 1988. Cryo-electron microscopy of vitrified specimens. *Quarterly Reviews of Biophysics* **21,** 129–228.

Dudkina NV, Heinemeyer J, Keegstra W, Boekema EJ, Braun HP. 2005. Structure of dimeric ATP synthase from mitochondria: an angular association of monomers induces the strong curvature of the inner membrane. *FEBS Letters* **579,** 5769–5772.

Dudkina NV, Kouril R, Bultema JB, Boekema EJ. 2010*a*. Imaging of organelles by electron microscopy reveals protein–protein interactions in mitochondria and chloroplasts. *FEBS Letters* **584,** 2510–2515.

Dudkina NV, Oostergetel GT, Lewejohann D, Braun HP, Boekema EJ. 2010*b*. Row-like organization of ATP synthase in intact mitochondria determined by cryo-electron tomography. *Biochimica et Biophysica Acta* **1797,** 272–277.

Falk H, Sitte P. 1963. Zellfeinbau Bei Plasmolyse.1. Der Feinbau Der Elodea-Blattzellen. *Protoplasma* **57,** 290–303.

Frank J. 2006. *Electron tomography: methods for three-dimensional visualization of structures in the cell*. Berlin: Springer.

Ghosh S, Hudak KA, Dumbroff EB, Thompson JE. 1994. Release of photosynthetic protein catabolites by blebbing from thylakoids. *Plant Physiology* **106,** 1547–1553.

Hansmann P, Sitte P. 1982. Composition and molecular structure of chromoplast globules of *Viola tricolor*. *Plant Cell Reports* **1,** 111–114.

Heslop Harrison J. 1963. Structure and morphogenesis of lamellar systems in grana-containing chloroplasts. 1. Membrane structure and lamellar architecture. *Planta* **60,** 243–260.

Horton P, Black MT. 1980. Activation of adenosine 5'-triphosphate-induced quenching of chlorophyll fluorescence by reduced plastoquinone—the basis of state-I–state-II transitions in chloroplasts. *FEBS Letters* **119,** 141–144.

Kaup MT, Froese CD, Thompson JE. 2002. A role for diacylglycerol acyltransferase during leaf senescence. *Plant Physiology* **129,** 1616–1626.

Kessler F, Schnell D, Blobel G. 1999. Identification of proteins associated with plastoglobules isolated from pea (Pisum sativum L.) chloroplasts. *Planta* **208,** 107–113.

Kirchhoff H, Haase W, Wegner S, Danielsson R, Ackermann R, Albertsson PA. 2007. Low-light-induced formation of semicrystalline photosystem II arrays in higher plant chloroplast. *Biochemistry* **46,** 11169–11176.

Kouril R, Oostergetel GT, Boekema EJ. 2011. Fine structure of granal thylakoid membrane organization using cryo electron tomography. *Biochimica et Biophysica Acta* in press.

Kreuz K, Dehesh K, Apel K. 1986. The light-dependent accumulation of the P700 chlorophyll alpha-protein of the photosystem-I reaction center in barley—evidence for translational control. *European Journal of Biochemistry* **159,** 459–467.

Leis A, Rockel B, Andrees L, Baumeister W. 2009. Visualizing cells at the nanoscale. *Trends in Biochemical Sciences* **34,** 60–70.

Lichtenthaler HK. 1968. Plastoglobuli and fine structure of plastids. *Endeavour* **27,** 144–149.

Lichtenthaler HK, Tevini M. 1970. Distribution of pigments, plastid quinones and plastoglobuli in different particle fractions obtained from sonicated spinach chloroplasts. *Zeitschrift für Pflanzenphysiologie* **62,** 33–50.

Machold O, Meister A, Sagromsky H, Hoyerhansen G, Wettstein DV. 1977. Composition of photosynthetic membranes of wild-type barley and chlorophyll b-less mutants. *Photosynthetica* **11,** 200–206.

Menke W. 1960. Das Allgemeine Bauprinzip des Lamellarsystems der Chloroplasten. *Experientia* **16,** 537–538.

Menke W. 1962. Structure and chemistry of plastids. *Annual Review of Plant Physiology and Plant Molecular Biology* **13,** 27–44.

Miller KR, Staehelin LA. 1976. Analysis of thylakoid outer surface-coupling factor is limited to unstacked membrane regions. *Journal of Cell Biology* **68,** 30–47.

Mustárdy L, Buttle K, Steinbach G, Garab G. 2008. The three-dimensional network of the thylakoid membranes in plants: quasihelical model of the granum–stroma assembly. *The Plant Cell* **20,** 2552–2557.

Mustárdy L, Garab G. 2003. Granum revisited. A three-dimensional model—where things fall into place. *Trends in Plant Science* **8,** 117–122.

Mustárdy LA, Janossy AGS. 1979. Evidence of helical thylakoid arrangement by scanning electron-microscopy. *Plant Science Letters* **16,** 281–284.

Nelson N, Ben-Shem A. 2004. The complex architecture of oxygenic photosynthesis. *Nature Reviews Molecular Cell Biology* **5,** 971–982.

Nevo R, Chuartzman SG, Tsabari O, Reich Z. 2009. Architecture of thylakoid membrane networks. In: Wada H, Murata N, eds. *Lipids in photosynthesis: essential and regulatory functions*. Berlin: Springer, 295–328.

Nield J, Barber J. 2006. Refinement of the structural model for the photosystem II supercomplex of higher plants. *Biochimica et Biophysica Acta* **1757,** 353–361.

Norlen L, Oktem O, Skoglund U. 2009. Molecular cryo-electron tomography of vitreous tissue sections: current challenges. *Journal of Microscopy-Oxford* **235,** 293–307.

Paolillo DJ. 1970. The three-dimensional arrangement of intergranal lamellae in chloroplasts. *Journal of Cell Science* **6,** 243–355.

Paumard P, Vaillier J, Coulary B, Schaeffer J, Soubannier V, Mueller DM, Brethes D, di Rago JP, Velours J. 2002. The ATP synthase is involved in generating mitochondrial cristae morphology. *EMBO Journal* **21,** 221–230.

Pierson J, Sani M, Tomova C, Godsave S, Peters PJ. 2009. Toward visualization of nanomachines in their native cellular environment. *Histochemistry and Cell Biology* **132,** 253–262.

PozuetaRomero J, Rafia F, Houlne G, Cheniclet C, Carde JP, Schantz ML, Schantz R. 1997. A ubiquitous plant housekeeping gene, PAP, encodes a major protein component of bell pepper chromoplasts. *Plant Physiology* **115,** 1185–1194.

Schermelleh L, Heintzmann R, Leonhardt H. 2010. A guide to super-resolution fluorescence microscopy. *Journal of Cell Biology* **190,** 165–175.

Shimoni E, Rav-Hon O, Ohad I, Brumfeld V, Reich Z. 2005. Three-dimensional organization of higher-plant chloroplast thylakoid membranes revealed by electron tomography. *The Plant Cell* **17,** 2580–2586.

Staehelin LA. 1975. Chloroplast membrane structure—intramembranous particles of different sizes make contact in stacked membrane regions. *Biochimica et Biophysica Acta* **408,** 1–11.

Staehelin LA. 1986. Chloroplast structure and supramolecular organization of photosynthetic membranes. In: Staehelin LA, Arntzen CJ, eds. *Photosynthesis III. Photosynthetic membranes and light harvesting systems*. Wallingford, UK: CABI Publishing, 1–84.

Staehelin LA. 2003. Chloroplast structure: from chlorophyll granules to supra-molecular architecture of thylakoid membranes. *Photosynthesis Research* **76,** 185–196.

Standfuss J, Terwisscha van Scheltinga AC, Lamborghini M, Kühlbrandt W. 2005. Mechanisms of photoprotection and nonphotochemical quenching in pea light-harvesting complex at 2.5 Å resolution. *EMBO Journal* **24,** 919–928.

Steinmüller D, Tevini M. 1985. Composition and function of plastoglobuli. 1. Isolation and purification from chloroplasts and chromoplasts. *Planta* **163,** 201–207.

Strauss M, Hofhaus G, Schröder RR, Kühlbrandt W. 2008. Dimer ribbons of ATP synthase shape the inner mitochondrial membrane. *EMBO Journal* **27,** 1154–1160.

Tevini M, Herm K, Leonhardt HD. 1977. Lipids and function of etiochloroplasts after UV, blue and red light-illumination. *Biochemical Society Transactions* **5,** 95–98.

Tevini M, Steinmüller D. 1985. Composition and function of plastoglobuli. 2. Lipid-composition of leaves and plastoglobuli during beech leaf senescence. *Planta* **163,** 91–96.

Tocheva E, Li Z, Jensen G. 2010. Electron cryotomography. *Cold Spring Harbor Perspectives in Biology* **2,** a003442.

Trissl HW, Wilhelm C. 1993. Why do thylakoid membranes from higher-plants form grana stacks. *Trends in Biochemical Sciences* **18,** 415–419.

van Roon H, van Breemen JFL, de Weerd FL, Dekker JP, Boekema EJ. 2000. Solubilization of green plant thylakoid membranes with n-dodecyl-alpha, d-maltoside. Implications for the structural organization of the photosystem II, photosystem I, ATP synthase and cytochrome b(6)f complexes. *Photosynthesis Research* **64,** 155–166.

Vidi PA, Kanwischer M, Baginsky S, Austin JR, Csucs G, Dormann P, Kessler F, Brehelin C. 2006. Tocopherol cyclase (VTE1) localization and vitamin E accumulation in chloroplast plastoglobule lipoprotein particles. *Journal of Biological Chemistry* **281,** 11225–11234.

Wehrmeyer W. 1964*a*. Über Membranbildungsprozesse im Chloroplasten. 2. Zur Entstehung der Grana durch Membranüberschiebung. *Planta* **63,** 13–30.

Wehrmeyer W. 1964*b*. Zur Klárung der Strukturellen Variabilitat der Chloroplastengrana des Spinats in Profil und Aufsicht. *Planta* **62,** 272–293.

Weier TE, Drever H, Thomson WW, Stocking CR. 1963. The grana as structural units in chloroplasts of mesophyll of *Nicotiana rustica* and Phaseolus vulgaris. *Journal of Ultrastructure Research* **8,** 122–143.

Wollenberger L, Stefansson H, Yu SG, Albertsson PA. 1994. Isolation and characterization of vesicles originating from the chloroplast grana margins. *Biochimica et Biophysica Acta* **1184,** 93–102.

Yao K, Paliyath G, Humphrey RW, Hallett FR, Thompson JE. 1991*a*. Identification and characterization of nonsedimentable lipid protein microvesicles. *Proceedings of the National Academy of Sciences, USA* **88,** 2269–2273.

Yao KN, Paliyath G, Thompson JE. 1991*b*. Nonsedimentable microvesicles from senescing bean cotyledons contain gel phase-forming phospholipid degradation products. *Plant Physiology* **97,** 502–508.

Ytterberg AJ, Peltier JB, van Wijk KJ. 2006. Protein profiling of plastoglobules in chloroplasts and chromoplasts. A surprising site for differential accumulation of metabolic enzymes. *Plant Physiology* **140,** 984–997.